Exciton effect in deformed carbon nanotubes

2007 J. Phys.: Condens. Matter 19 266222

(http://iopscience.iop.org/0953-8984/19/26/266222)

IOP PUBLISHING JOURNAL OF PHYSICS: CONDENSED MATTER

J. Phys.: Condens. Matter **19** (2007) 266222 (10pp) doi:10.1088/0953-8984/19/26/266222

Exciton effect in deformed carbon nanotubes

Guili Yu, Yonglei Jia and Jinming Dong[1]

Group of Computational Condensed Matter Physics, National Laboratory of Solid State Microstructures and Department of Physics, Nanjing University, Nanjing 210093, People's Republic of China

E-mail: jdong@nju.edu.cn

Received 9 March 2007, in final form 30 May 2007
Published 15 June 2007
Online at stacks.iop.org/JPhysCM/19/266222

Abstract

The exciton states in deformed single-walled carbon nanotubes (SWNTs), under two kinds of strain, i.e., uniaxial and torsional, are theoretically studied in the Su–Schrieffer–Heeger (SSH) model, supplemented by long-range Coulomb interactions. It is found that for semiconducting zigzag tubes, the exciton binding energy E_b and the (quasi-)continuum edge E_c are very sensitive to the uniaxial strain, but not to the torsional one, showing two different kinds of variation behaviour of E_b with increasing uniaxial strain, of which one decreases monotonically, and the other first increases and then decreases. Additionally, the excitons in torsionally distorted armchair tubes and uniaxially strained metallic zigzag tubes have also been studied, showing increased E_b and E_c with increasing strain.

(Some figures in this article are in colour only in the electronic version)

1. Introduction

Since the discovery [1] of carbon nanotubes (CNTs) in 1991 by Iijima, there has been much interest in their physical and chemical properties, especially their optical properties, which are of great importance and practical interest because from them we can get some information of the CNTs' geometrical and electrical structures. Their optical absorption and emission spectra have been studied experimentally and theoretically by a number of groups [2–7]. Recently, a consensus [8, 9] emerged that the optical absorptions in semiconducting SWNTs are greatly affected by the excitons, which play an important role in one-dimensional (1D) systems, such as semiconductor quantum wires [10] and conjugated polymers [11, 12].

The exciton effect on the optical properties of semiconducting CNTs has been theoretically studied by different methods, such as the tight-binding method, variational calculations [13–15] and the *ab initio* solution of the Bethe–Salpeter equation (BSE) [7, 16], finding that the exciton

[1] Author to whom any correspondence should be addressed.

binding energy E_b varies inversely with the diameters of the CNTs. Experimentally, there exists growing evidence [17, 18] that the absorption and photoluminescence (PL) peaks in the CNTs are excitonic in character. Their E_b has been measured [19] from two-photon excitation spectroscopy, showing the same dependence on the tube diameter and chiral angle as predicted by theoretical calculations.

However, the SWNTs are usually supported on a solid substrate in experiments, causing various mechanical deformations. An applied uniaxial or torsional strain can also induce SWNT deformations, changing their electronic structures and corresponding transport and optical properties [20–29]. For example, the energy level degeneracy may be destroyed by the symmetry breaking induced by the deformations, and the σ–π mixing could be enhanced by the increased curvature. A metal–semiconductor transition of the SWNTs could be induced by the deformation. Because of the fundamental importance of the deformed CNTs and their promising potential applications in future nano-electromechanical devises, there have been a lot of theoretical and experimental researches on the electronic, transport and optical properties of the deformed CNTs [20–29]. Several theoretical studies on the π-electronic structures of deformed SWNTs under two kinds of strain, i.e., the uniaxial and torsional [28, 29], have shown that the band structures of the deformed SWNTs are determined by their chiral symmetries and the kind of strain; for example, their band gap varies with increasing strain, depending on their chiral angles. Their optical properties [20] are also very sensitive to the kind of strain and the CNT geometry. The metal–semiconductor transition of torsional metallic SWNTs, as predicted theoretically, has been observed experimentally [30].

However, up to now, there has been no discussion on the exciton effect in the deformed CNTs. So, it is very interesting to know the influence of applied strains on the exciton binding energy E_b and its (quasi-)continuum edge E_c of semiconducting CNTs, which could find applications in future nano-optical and nano-optical–mechanical coupling devices. In this work, we have studied the excitons in armchair and zigzag SWNTs under uniaxial and torsional strains. It is found that the E_b and E_c of semiconducting zigzag tubes depend sensitively on the kind of strain and their chiral angles.

The paper is organized as follows. The model and calculation method used in this paper are discussed in section 2. The obtained results and discussions are given in section 3. The conclusions are presented in section 4.

2. Model and method

The Hamiltonian of deformed SWNTs studied here is the SSH tight-binding one:

$$H = \sum_{\langle i,j\rangle,s} t_{ij} C^{\dagger}_{i,s} C_{j,s} + \text{H.c.} \tag{1}$$

where $C^{\dagger}_{i,s}(C_{j,s})$ is the creation (annihilation) operator of an electron at site $i(j)$ with spin s. The nearest-neighbour hopping parameter $t_{i,j}(< 0)$ depends on the bond length, which is assumed to be $t_{i,j} = t_0(r_0/r_{ij})^2$ with r_{ij} the deformed bond length between site i and j [28]. r_0 and t_0 are the bond length and hopping parameter of the SWNTs without deformations, respectively. Here, t_0 is chosen to be -2.0 eV, which has been used successfully in [31]. The uniaxial and torsional strains will cause the following changes of the bond vectors:

$$r_{it} \to (1 + \epsilon_t), \qquad \text{and,} \qquad r_{ic} \to (1 + \epsilon_c) \text{ (tensile)}, \tag{2}$$

$$r_{ic} \to r_{ic} + \tan(\gamma) r_{it} \text{ (torsion)}, \tag{3}$$

where $i = 1, 2, 3$ and r_{ip} is the p component of the $\vec{r}_i$ (p = c, t. Here, t and c denote the tube

axis and circumference direction, respectively). ϵ_t and ϵ_c represent the uniaxial strain along $\widehat{t}$ and $\widehat{c}$, respectively. γ is the shear strain.

We perturb the Hamiltonian H_0 with the electron–electron Coulomb interactions H_1, which are described by the following model:

$$H_{e-e} = U \sum_i n_{i,\uparrow} n_{i,\downarrow} + \frac{1}{2} \sum_{i,j} V_{ij}(n_i - 1)(n_j - 1). \tag{4}$$

Here, $n_i = \sum_s C^\dagger_{i,s} C_{i,s}$ is the total number of π electrons on site i. The parameters U and V_{ij} are the on-site and inter-site Coulomb interactions. In the actual calculations, the long-range V_{ij} is taken to be the standard Ohno parameterization [32, 33], i.e.,

$$V_{ij} = \frac{U}{\kappa \sqrt{1 + 0.6117 r_{ij}^2}}. \tag{5}$$

Here, r_{ij} is measured in units of Å, and κ is a screening parameter. We have made calculations of deformed semiconducting zigzag tubes for $\frac{U}{|t_0|} = 1.9, 2.5, 2.9, 3.33, 4.0$ and $\kappa = 1, 2$, obtaining very similar qualitative results in all the cases. So, in this paper, we report only the calculation results for $\frac{U}{|t_0|} = 4.0$ and $\kappa = 2$, which have also been used in [31]. However, for the deformed metallic tubes, the screening parameter should be larger [34], and we increase the screening parameter up to 5.

According to the standard exciton theory [35], we choose the single electron states of H_0 as the basis and construct a set of single electron–hole (e–h) pair excitation states from the ground state $|g\rangle$:

$$|k_c, k_v\rangle = \frac{1}{\sqrt{2}}(C^\dagger_{k_c\uparrow} C_{k_v\uparrow} \pm C^\dagger_{k_c\downarrow} C_{k_v\downarrow})|g\rangle \tag{6}$$

where '+' denotes the spin singlet and '−' the spin triplet state, and k_c and k_v are wavenumbers along the tube axis in the conduction and valence band states, respectively. Then the matrix of the Hamiltonian $H = H_0 + H_1$ within the single e–h excitation subspace is calculated and diagonalized, which has to be carried out numerically in actual calculations for a finite-length CNT. It is known that the wavenumber $k_\perp$ in the direction of the circumference is quantized as $k_\perp = 2\pi q / c_h a_0$ ($q = 0, 1, \ldots, n_c - 1$). Here, n_c is the number of hexagons in a 1D unit cell of the tube. $a_0 = |\vec{a}_1| = |\vec{a}_2| = 2.46$ Å is the length of unit vector in graphite. $c_h = \sqrt{n^2 + nm + m^2}$ is the circumference length of the (n, m) tube in units of a_0. If one takes into account the effect of finite tube length, the axial wavenumber of $k_c(k_v)$ is also quantized as $k_{c(v)} = 2\pi j / L T_0$ (j is an integer, $-\frac{L}{2} \leqslant j < \frac{L}{2}$). Here, L is the tube length in units of T_0, the length of the translational unit cell of the 1D infinite SWNT. We now can assume $k_c = k + K$ and $k_v = k - K$, where k is the relative momentum of the e–h pair and K is the momentum of the mass centre of the e–h pair. Thus, the state $|k_c, k_v\rangle$ can be represented by the state $|k, K\rangle$. In the single e–h pair excitation states $|k, K\rangle$, the matrix elements of the excitation Hamiltonian of $(H - E_0)$ in the spin singlet ($\delta_s = 1$) and triplet ($\delta_s = 0$) states can be written as [11, 12, 36]

$$\begin{aligned}\langle k', K'|(H - E_0)|k, K\rangle = {} & \delta_{K',K}\{\delta_{k',k}[\widetilde{\epsilon}_c(k + K) - \widetilde{\epsilon}_v(k - K)] \\ & + 2\delta_s W_x(k, k', K) - W_c(k, k', K)\}.\end{aligned} \tag{7}$$

Here, $E_0 = \langle g|H|g\rangle$ represents the expectation value of H in the ground state $|g\rangle = \prod_{k_v} C^\dagger_{k_v,\uparrow} C^\dagger_{k_v,\downarrow}|0\rangle$ with $|0\rangle$ the vacuum state without electrons. $\widetilde{\epsilon}_c$ and $\widetilde{\epsilon}_v$ are the energies of one-electron states in the conduction and the valence bands, respectively, which include the first-order energy corrections concerning the Coulomb interactions. Their explicit forms are given as follows.

$$\widetilde{\epsilon}_c = \epsilon_c + \Delta\epsilon_c, \widetilde{\epsilon}_v = -\widetilde{\epsilon}_c, \tag{8}$$

$$\epsilon_c = \left\{ t_1^2 + t_2^2 + t_3^2 + 2t_1t_2\cos\left(\pi q\frac{n+2m}{c_h^2} - \frac{\sqrt{3}}{2}\frac{n}{c_h}k_c(1+\epsilon_t)a_0 - \pi q\frac{\sqrt{3}\tan(\gamma)}{1+\epsilon_c}\frac{n}{c_h^2}\right)\right.$$
$$+ 2t_1t_3\cos\left(\pi q\frac{2n+m}{c_h^2} + \frac{\sqrt{3}}{2}\frac{m}{c_h}k_c(1+\epsilon_t)a_0 + \pi q\frac{\sqrt{3}\tan(\gamma)}{1+\epsilon_c}\frac{m}{c_h^2}\right)$$
$$\left. + 2t_2t_3\cos\left(\pi q\frac{n-m}{c_h^2} + \frac{\sqrt{3}}{2}\frac{n+m}{c_h}k_c(1+\epsilon_t)a_0 + \pi q\frac{\sqrt{3}\tan(\gamma)}{1+\epsilon_c}\frac{n+m}{c_h^2}\right)\right\}^{\frac{1}{2}} \tag{9}$$

$$\Delta\epsilon_{k_c} = \frac{1}{LN_c}\sum_p\sum_{gh} e^{i(\vec{p}-\vec{k}-\vec{K})\cdot\vec{r}} \times [V_{12}(g,h)\xi_{k+K}\xi_p^*\xi_p^*\xi_{k+K} + V_{21}(g,h)\xi_{k+K}^*\xi_p\xi_p\xi_{k+K}^*]. \tag{10}$$

Here, V_{ij} denotes the electron–electron interaction between the i_{th} carbon atom in the graphite unit cell (g, h) and the j_{th} one in the graphite unit cell (0, 0). $\xi_k = (h_0/2|h_0|)^{\frac{1}{2}}$, and the expression of h_0 is given as follows:

$$h_0 = t_1 + t_2 e^{-i(\pi q\frac{n+2m}{c_h^2} - \frac{\sqrt{3}n}{2c_h}k_c(1+\epsilon_t)a_0 - \pi q\frac{\sqrt{3}\tan\gamma}{1+\epsilon_c}\frac{n}{c_h^2})} + t_3 e^{-i(\pi q\frac{2n+m}{c_h^2} + \frac{\sqrt{3}m}{2c_h}k_c(1+\epsilon_t)a_0 + \pi q\frac{\sqrt{3}\tan\gamma}{1+\epsilon_c}\frac{m}{c_h^2})}. \tag{11}$$

In equation (7), the Coulomb part W_c and the exchange part W_x are given as follows:

$$W_c = \frac{1}{LN_c}\sum_{gh} e^{i(\vec{k}-\vec{k'})\cdot\vec{r}} \times [V_{12}(g,h)\xi_{k'+K}\xi_{k+K}^*\xi_{k'-K}\xi_{k-K}^* + V_{11}(g,h)\xi_{k'+K}\xi_{k+K}^*\xi_{k'-K}^*\xi_{k-K}$$
$$+ V_{21}(g,h)\xi_{k'+K}^*\xi_{k+K}\xi_{k'-K}^*\xi_{k-K} + V_{22}(g,h)\xi_{k'+K}^*\xi_{k+K}\xi_{k'-K}\xi_{k-K}^*] \tag{12}$$

$$W_x = \frac{1}{LN_c}\sum_{gh}\{V_{11}(g,h)\xi_{k'+K}\xi_{k+K}^*\xi_{k'-K}^*\xi_{k-K} + V_{22}(g,h)\xi_{k'+K}^*\xi_{k+K}\xi_{k'-K}\xi_{k-K}^*$$
$$- [V_{12}(g,h)\xi_{k'+K}\xi_{k+K}\xi_{k'-K}^*\xi_{k-K}^* + V_{21}(g,h)\xi_{k'+K}^*\xi_{k+K}^*\xi_{k'-K}\xi_{k-K}]\}. \tag{13}$$

If the system has spatial inversion symmetry, the exciton space can be divided into two subspaces: antisymmetric B_u states $|k;+K\rangle[\equiv (|k,K\rangle + |-k,K\rangle)/\sqrt{2}]$ and symmetric A_g states $|k;-K\rangle[\equiv (|k,K\rangle - |-k,K\rangle)/\sqrt{2}]$ [11, 12]. Considering the symmetry, the matrix elements of the excitation Hamiltonian in both B_u and A_g subspaces can be written in the following form:

$$\langle k';\pm,K|(H-E_0)|k;\pm,K\rangle = \delta_{k',k}[\widetilde{\epsilon_c}(k+K) - \widetilde{\epsilon_v}(k-K)]$$
$$+ 2\delta_s W_x(k',k;\pm,K) - W_c(k',k;\pm,K). \tag{14}$$

Here,

$$W_x(k',k;+,K) = 2W_x(k',k;K) \tag{15}$$
$$W_c(k',k;+,K) = W_c(k',k;K) + W_c(k',-k;K) \tag{16}$$
$$W_x(k',k;-,K) = 0 \tag{17}$$
$$W_c(k',k;-,K) = W_c(k',k;K) - W_c(k',-k;K). \tag{18}$$

It is clearly seen from the above equations that all the A_g states, including the singlet and triplet states, are degenerate.

3. Results and discussions

Now, we first discuss the exciton effect in semiconducting zigzag tubes under uniaxial and torsional strains, and then in torsional armchair tubes and uniaxially strained metallic zigzag ones, both of which can be transformed into semiconducting SWNTs. The tube length is taken

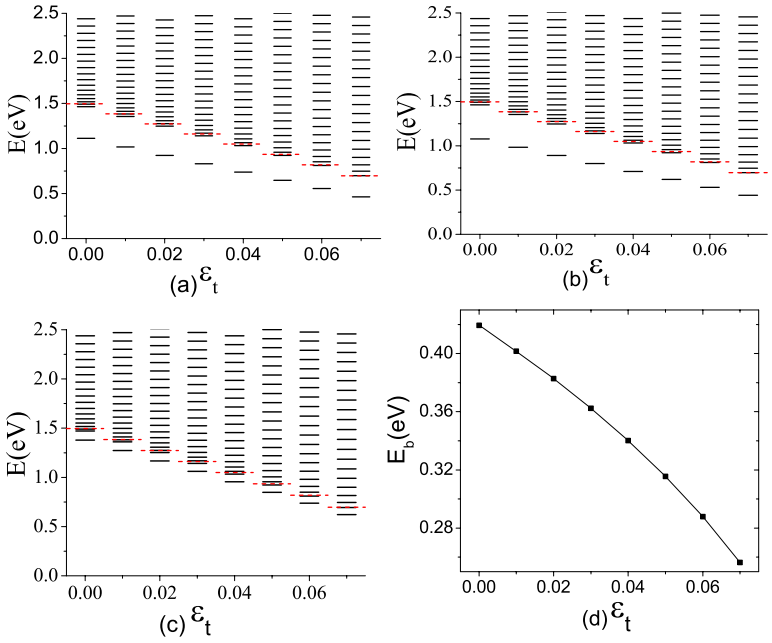

Figure 1. Calculated excitation energy levels of the (11, 0) tube at $K = 0$, $L = 180$ for the first subbands nearest the Fermi level versus uniaxial strain in different states: (a) ^1B_u state, (b) ^3B_u state, and (c) degenerate A_g state. (d) Variation of E_b in the ^3B_u state with increasing uniaxial strain. The dashed lines denote E_c.

to be $180T_0$, and the periodical boundary condition along the tube axis is used to avoid the finite-length effect. The band index q in our calculations is limited to the bands nearest to the Fermi level for the first subband transitions, associated with the transitions between the highest valence subband and the lowest conduction subband in semiconducting SWNTs.

3.1. Semiconducting zigzag tubes

According to [28], the band gap of semiconducting zigzag tubes is very sensitive to uniaxial strain but has only a small change under torsional strain. In the case of uniaxial strain, the band gap of zigzag tubes depends on the value of $(n - m)$ mod 3. When the value equals -1, the band gap will decrease with increasing strain, while for the value of 1, it will first increase and then decrease with increasing strain. Here, we take only (10, 0) and (11, 0) tubes as an example, both of which have different values of $(n-m)$ mod 3. As is well known, uniaxial strain does not destroy the inversion symmetry of zigzag tubes [37], so we can still calculate their E_b and E_c in the B_u and A_g subspaces under the applied uniaxial strain. Note that E_c equals the minimum of the renormalized one-electron excitation energy, $\widetilde{\epsilon}_c(k + K) - \widetilde{\epsilon}_v(k - K)$. In general, the states below and above E_c can be defined as exciton states and unbound electron–hole states, respectively, although the distinction between them may not be absolutely strict, especially near E_c, because of the finiteness of the system.

The excitation energies of the (11, 0) tube in the ^1B_u, ^3B_u and A_g states, varying with increase of the uniaxial strain, are given in figure 1; the ^3B_u state is the lowest exciton energy state. At $\epsilon_t = 0$, the E_b of the (11, 0) tube in the ^3B_u state is found to be about 0.419 eV, which is in excellent agreement with the earlier studies [17, 31, 32]. From figures 1(a)–(c), it is seen clearly that E_c decreases with increasing strain, which is consistent with the change of band

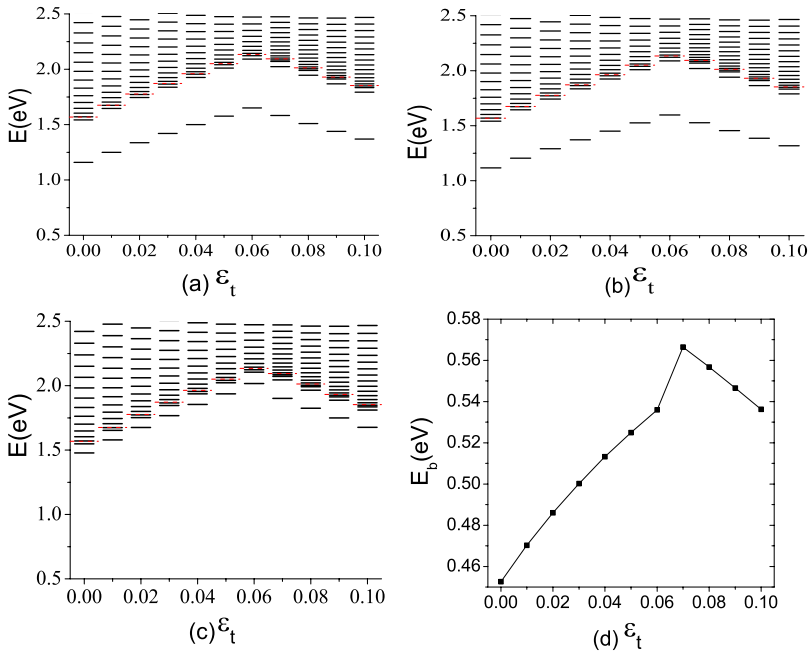

Figure 2. Calculated excitation energy levels of the (10, 0) tube at $K = 0$, $L = 180$ for the first subbands nearest the Fermi level versus uniaxial strain in different states: (a) ^1B_u state, (b) ^3B_u state, and (c) degenerate A_g state. (d) Variation of E_b in the ^3B_u state with increasing uniaxial strain. The dashed lines denote E_c.

gap. The variation of E_b in the ^3B_u state of the (11, 0) tube with increase of the uniaxial strain is given in figure 1(d), also showing a decrease with increasing strain. The variation slope of $dE_b/d\epsilon_t$ is found to be almost a constant, which is about 2.30 eV in the ^3B_u state. Of course, E_b in the ^1B_u and A_g states can also be obtained; its variation with increasing strain is similar to that in the ^3B_u state. However, $dE_b/d\epsilon_t$ in the ^1B_u and A_g states is, respectively, slightly smaller and three times smaller than that in the ^3B_u state. From the variation slopes of $dE_b/d\epsilon_t$, we can conclude that the uniaxial strain has the greatest influence on E_b in the ^3B_u state.

The same numerical calculation has been made for the (10, 0) tube in both B_u and A_g subspaces, and the results obtained are displayed in figure 2. In contrast to figure 1, E_c now first increases and then decreases with increase of the strain, which is caused by the change of band index q corresponding to the lowest excitation energies, and could be understood by the change of band gap. For the (10, 0) tube, the reversal point of the variation slope, $dE_b/d\epsilon_t$, lies between $\epsilon_t = 0.06$ and 0.07. The variation of E_b with increase of strain in the ^3B_u state is given in figure 2(d), showing first an increase and then a decrease, but also the existence of a jump of $\sim$0.03 eV at the reversal point, which is completely different from that shown in figure 1(d) for the (11, 0) tube. That is because both (11, 0) and (10, 0) semiconducting zigzag tubes have different values of $(n - m)$ mod 3, among which the former has a -1 value of $(n - m)$ mod 3, but the latter has $+1$. The same variation behaviour with increasing strain for E_b and the slope $dE_b/d\epsilon_t$ can be obtained in both ^1B_u and A_g states.

It is known that the band gap of semiconducting zigzag tubes is insensitive to torsional strain. From our calculations, we get the same conclusion that the torsional strain leads to a small change of their E_c and E_b. Due to the symmetry breaking under the torsional strain [37], the calculation has to be done for the singlet and triplet states.

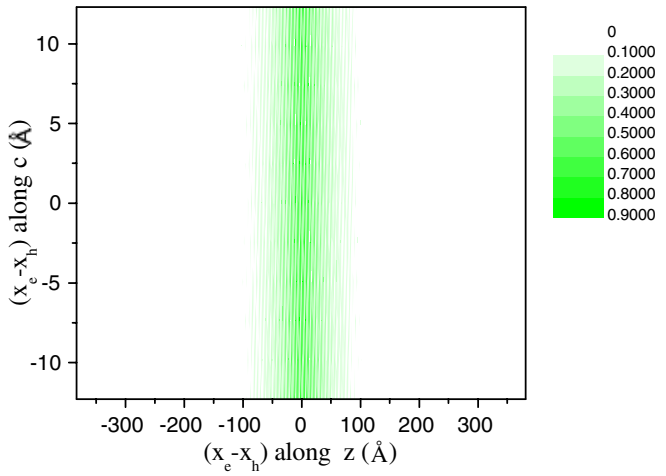

Figure 3. The exciton wavefunction of the (11, 0) tube in the first ^1B_u state under a uniaxial strain ($\epsilon_t = 0.01$). The colour (greyscale) plot represents the probability of finding a hole for the fixed electron position at the origin of the coordinate system. Here, z represents the tube axis direction, and c the circumference direction.

What is the effect of the applied strains on the exciton size in the SWNTs? Here, we have only taken the first ^1B_u exciton state of the (11, 0) tube as an example, and plotted in figure 3 its exciton wavefunction $\psi(x_e, x_h)$ under a uniaxial strain $\epsilon_t = 0.01$ by fixing the electron position at the origin of the coordinate system. From figure 3, it is clearly seen that the exciton is localized in the tube axis direction, but is delocalized along the tube circumference, indicating that this ^1B_u state is a bound exciton state, which is in an agreement with [8] and [14]. The influence of increasing strain on the exciton wavefunction of the first ^1B_u state is shown in figure 4(a), in which the wavefunction has been averaged over the circumference direction. It is seen from figure 4(a) that with increasing strain ϵ_t, the wavefunction becomes less localized along the tube axis. The exciton size d along the tube axis can be obtained from the formula $d = \sqrt{\langle (x_e - x_h)^2 \rangle}$, from which the exciton size varying with increasing strain can be obtained; it is given in figure 4(b), also showing clearly the delocalization effect caused by the applied uniaxial strain. For example, the exciton size is 25.2 Å in the case of no applied strain, but when ϵ_t increases to 0.07, the size increases about one and half times, reaching 37.4 Å.

3.2. Torsionally distorted armchair tube and uniaxially strained metallic zigzag tube

A metal–semiconductor transition may occur for an armchair tube under torsional strain and a metallic zigzag one under uniaxial strain. Hence, these two kinds of metallic tube could be changed into semiconducting ones, and a band gap be opened by the strains. So, it is of great interest to discuss the exciton effect in these deformed metallic carbon nanotubes. As an example, we have studied the exciton effect in the torsional armchair (10, 10) tube and the uniaxial metallic zigzag (9, 0) tube. The results obtained are given, respectively, in figures 5 and 6. It is found from them that E_c and E_b increase with increasing strain in these two cases, which is consistent with their band gap variations. However, it is known by comparison that the E_b of these two tubes under applied strain are much smaller than those of the deformed semiconducting SWNTs, showing a much different effect of the deformations on the excitons in semiconducting and metallic SWNTs.

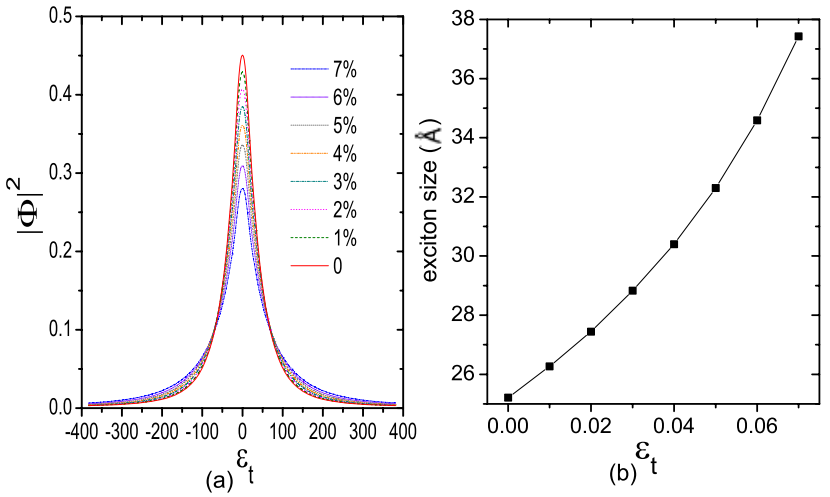

Figure 4. (a) Exciton wavefunction in the first ^1B_u state of the (11, 0) tube under different uniaxial strains, averaged over the circumference direction. (b) The exciton size in the first ^1B_u state of the (11, 0) tube versus the uniaxial strain ϵ_t.

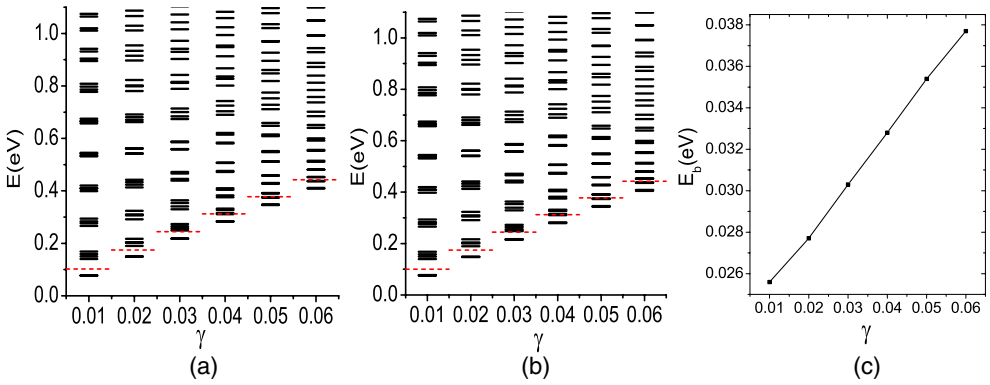

Figure 5. Calculated excitation energy levels and E_b of the armchair (10, 10) tube at $K = 0$, $L = 180$ for the bands nearest to the Fermi level versus the torsional strain γ in different states: (a) singlet state, (b) triplet state. (c) Variation of E_b in the triplet state with γ. The dashed lines denote E_c.

Using the same method, we can also study their exciton wavefunctions under applied strain. Here, we take the first ^1B_u exciton state of the zigzag (9, 0) tube as an example, and show in figure 7 the strain influence on its exciton wavefunction averaged over the circumference direction. It is seen from figure 7 that, in this case, the strain influence on the exciton wavefunction of the zigzag (9, 0) tube is different from that in the semiconducting zigzag (11, 0) tube, shown in figure 4(a). With increasing strain, the exciton wavefunction now becomes increasingly localized in the tube axis because its band gap now increases with increasing strain.

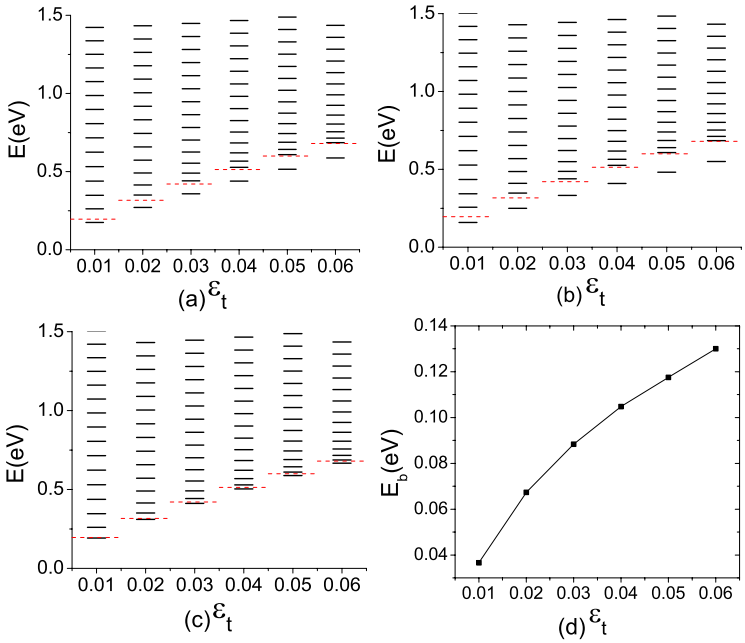

Figure 6. Calculated excitation energy levels of the (9, 0) tube at $K = 0, L = 180$ for the first subbands nearest the Fermi level versus uniaxial strain in different states: (a) ^1B_u state, (b) ^3B_u state, and (c) degenerate A_g state. (d) Variation of E_b in the ^3B_u state with increasing uniaxial strain. The dashed lines denote E_c.

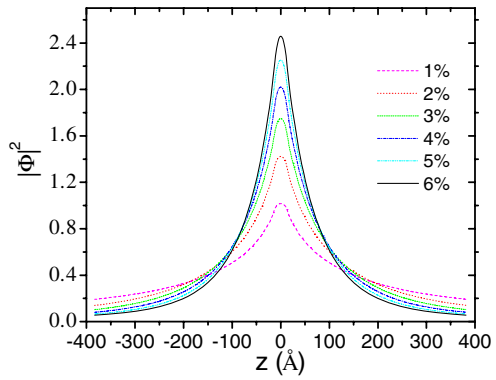

Figure 7. Exciton wavefunction in the first ^1B_u state of a metallic (9, 0) tube under different uniaxial strains, averaged over the circumference direction.

4. Conclusions

In summary, we have used the simple SSH model Hamiltonian supplemented by long-range Coulomb interactions to study the exciton effect in deformed SWNTs under applied uniaxial and torsional strains. Values of E_c and E_b have first been calculated for semiconducting (10, 0) and (11, 0) SWNTs under uniaxial and torsional strains, showing that all of them are sensitive to uniaxial strain, but not to torsional strain. As the uniaxial strain increases, the E_c, E_b change in two different ways: (a) both of them decrease for type I tubes with their values of $(n - m)$

mod 3 being -1; (b) both of them first increase and then decrease at a critical uniaxial strain value for type II tubes with their values of $(n-m)$ mod 3 being 1. The excitons in the torsional armchair (10, 10) tube and uniaxially strained metallic zigzag (9, 0) tube have also been studied, showing that their E_c and E_b increase with increasing strain.

Acknowledgments

This work was supported by the Natural Science Foundation of China under Grant Nos 10474035 and A040108, and also from a Grant for State Key Program of China through Grant No. 2004CB619004.

References

[1] Jijima S 1994 *Nature* **354** 56
[2] Li Z M, Tang Z K, Liu H J, Wang N, Chan C T, Saito R, Okada S, Li G D, Chen J S, Nagasawa N and Tsuda S 2001 *Phys. Rev. Lett.* **87** 127401
[3] Bachilo S M, Strano M S, Kittrell C, Hauge R H, Smalley R E and Weisman R B 2002 *Science* **298** 2361
[4] Hagen A and Hertel T 2003 *Nano Lett.* **3** 383
[5] Lebedkin S, Hennrich F, Skipa T and Kappes M M 2003 *J. Phys. Chem.* B **107** 1949
[6] Lefebvre J, Homma Y and Finnie P 2003 *Phys. Rev. Lett.* **90** 217401
[7] Spataru C D, Ismail-Beigi S, Benedict L X and Louie S G 2004 *Phys. Rev. Lett.* **92** 077402
[8] Chang E, Bussi G, Ruini A and Molinari E 2004 *Phys. Rev. Lett.* **92** 196401
[9] Perebeinos V, Tersoff J and Avouris P 2004 *Phys. Rev. Lett.* **92** 257402
[10] Rossi F and Molinari E 1996 *Phys. Rev. Lett.* **76** 3642
[11] Abe S, Yu J and Su W P 1992 *Phys. Rev.* B **45** 8264
[12] Zhao H, Fu R T, Sun X and Zhang Z L 1997 *Phys. Rev.* B **56** 12268
[13] Kane C L and Mele E J 2003 *Phys. Rev. Lett.* **90** 207401
[14] Pedersen T G 2003 *Phys. Rev.* B **67** 073401
[15] Pedersen T G 2004 *Carbon* **42** 1007
[16] Spataru C D, Ismail-Beigi S, Benedict L X and Louie S G 2004 *Appl. Phys.* A **78** 1129
[17] Wang F, Dukovic G, Brus L E and Heinz T F 2005 *Science* **308** 838
[18] Maultzsch J, Pomraenke R, Reich S, Chang E, Prezzi D, Ruini A, Molinari E, Strano M S, Thomsen C and Lienau C 2005 *Phys. Rev.* B **72** 241402(R)
[19] Dukovic G, Wang F, Song D H, Sfeir M Y, Heinz T F and Brus L E 2005 *Nano Lett.* **5** 2314
[20] Jiang H, Wu G, Yang X and Dong J 2004 *Phys. Rev.* B **70** 125404
[21] Heyd R, Charlier A and McRae E 1997 *Phys. Rev.* B **55** 6820
[22] Brenner D W, Schall J D, Mewkill J P, Shenderova D A and Sinnott S B 1998 *Interplanet. Soc.* **51** 137
[23] Kane C L and Mele E J 1997 *Phys. Rev. Lett.* **78** 1932
[24] Zhou J, Weng H M, Wu G and Dong J 2006 *Appl. Phys. Lett.* **89** 013102
[25] Bu W, Jiang J and Dong J 2002 *Phys. Lett.* A **302** 125
[26] Zhang Y, Yu G L and Dong J 2006 *Phys. Rev.* B **73** 205419
[27] Jiang H, Zhang Y, Yu G L and Dong J 2006 *Phys. Lett.* A **351** 308
[28] Yang L, Anantram M P, Han J and Lu J P 1999 *Phys. Rev.* B **60** 13874
[29] Yang L and Han J 2000 *Phys. Rev. Lett.* **85** 154
[30] Clauss W, Bergerom D J and Johnson A T 1998 *Phys. Rev.* B **58** R4266
[31] Wang Z D, Zhao H B and Mazumdar S 2006 *Phys. Rev.* B **74** 195406
[32] Zhao H and Mazumdar S 2004 *Phys. Rev. Lett.* **93** 157402
[33] Ohno K 1964 *Theor. Chim. Acta* **2** 219
[34] Kozinsky B and Marzari N 2006 *Phys. Rev. Lett.* **96** 166801
[35] Knox R S 1963 *Solid State Physics* (New York: Academic) Suppl. 5
[36] Harigaya K and Abe S 1994 *Phys. Rev.* B **49** 16746
[37] Wu G, Zhou J and Dong J 2005 *Phys. Rev.* B **72** 115411